International Journal of Biological Macromolecules 164 (2020) 4348–4358

Contents lists available at ScienceDirect

International Journal of Biological Macromolecules

journal homepage: http://www.elsevier.com/locate/ijbiomac

Structural features and antioxidant activities of Chinese quince (*Chaenomeles sinensis*) fruits lignin during auto-catalyzed ethanol organosolv pretreatment

Xi-Chuang Cheng [a], Xin-Ran Guo [b], Zhao Qin [a,*], Xue-De Wang [a], Hua-Min Liu [a,*], Yu-Lan Liu [a]

[a] College of Food Science and Technology, Henan University of Technology, Zhengzhou 450001, China
[b] School of International Education, Henan University of Technology, Zhengzhou 450001, China

ARTICLE INFO

Article history:
Received 20 June 2020
Received in revised form 24 August 2020
Accepted 31 August 2020
Available online 12 September 2020

Keywords:
Chinese quince fruit
Organosolv pretreatment
Lignin characterization

ABSTRACT

Chinese quince fruits (*Chaenomeles sinensis*) have an abundance of lignins with antioxidant activities. To facilitate the utilization of Chinese quince fruits, lignin was isolated from it by auto-catalyzed ethanol organosolv pretreatment. The effects of three processing conditions (temperature, time, and ethanol concentration) on yield, structural features and antioxidant activities of the auto-catalyzed ethanol organosolv lignin samples were assessed individually. Results showed the pretreatment temperature was the most significant factor; it affected the molecular weight, S/G ratio, number of β-O-4′ linkages, thermal stability, and antioxidant activities of lignin samples. According to the GPC analyses, the molecular weight of lignin samples had a negative correlation with pretreatment temperature. 2D-HSQC NMR and Py-GC/MS results revealed that the S/G ratios of lignin samples increased with temperature, while total phenolic hydroxyl content of lignin samples decreased. The structural characterization clearly indicated that the various pretreatment conditions affected the structures of organosolv lignin, which further resulted in differences in the antioxidant activities of the lignin samples. These results can be helpful for controlling and optimizing delignification during auto-catalyzed ethanol organosolv pretreatment, and they provide theoretical support for the potential applications of Chinese quince fruits lignin as a natural antioxidant in the food industry.

1. Introduction

Lignin is the most abundant natural phenolic polymer. It has an amorphous, highly branched, complex chemical structure. It is mainly composed of three different monomeric units, i.e. hydroxyphenyl (H), syringyl (S), and guaiacyl (G) units, which are chemically cross-linked by carbon-carbon, alkyl-ether, and aryl-ether bonds [1]. Many studies have revealed that lignin has significant antioxidant activity, and explored its potential application as a natural antioxidant in different products, such as cosmetics, pharmaceutical preparations, and foods [2,3]. Antioxidant activities of lignin polymers are directly correlated to the capability of their phenolic moieties to capture and neutralize free radicals. Catignani and Carter [4] reported that lignin could effectively delay the oxidation of corn oil. Ugartondo et al. [5] evaluated the cytotoxic effects of lignin samples from different sources, and found that, while exhibiting high antioxidant activity, these lignins were not harmful to normal human cells over a range of concentrations. However, the source of lignocellulosic materials, the extraction methods employed, and the treatments applied during its separation and purification strongly influence the antioxidant activity of the extracted lignins [6–8]. In addition, the antioxidant activity of certain lignins depends highly on their structure, particularly molecular weight and polydispersity. Lignins with low molecular weight and narrow polydispersity tend to exhibit high antioxidant activity [9,10].

Organosolv is an efficient process to produce a high-quality (free of sulfur and other inorganic impurities), low molecular weight (M_w) lignin. Its use may lead to new, multidimensional opportunities for the application of lignin [11,12]. Traditionally, the addition of catalysts (e.g. H_2SO_4) is a general option for higher organosolv delignification. However, the addition of catalysts may result in equipment corrosion, and their use also entails additional work for recovery and recycling, which affects the economy of the whole process, and even impedes the potential high valued-added utilization of lignin [13]. To facilitate upgrading the utilization of lignin and to reduce production costs, the auto-catalyzed ethanol organosolv pretreatment (AEOP) process has been developed [11]. During AEOP, organic acid hydrolyzed from the acetyl groups of arabinoxylans is used to enhance the dissociation of carbohydrates and dissolution of lignin [14]; therefore, there is no need for additional catalysts.

* Corresponding authors.
E-mail addresses: qinzhao505@163.com (Z. Qin), liuhuamin5108@163.com (H.-M. Liu).

https://doi.org/10.1016/j.ijbiomac.2020.08.249
0141-8130/

Chinese quince (*Chaenomeles sinensis*) (Rosaceae) is mainly cultivated in China, Japan, and Korea. Its fruits can be used as a Chinese traditional medicine to treat diseases, such as influenza, cough, and asthma. However, it is unpalatable because of its high content of lignin (24.5% of dry-weight) [15]. Thus, Chinese quince fruits is only consumed after processing in the form of jam, starch syrup, fruits liquor, wine and jelly [16,17].

Compared with the traditional lignocellulosic source materials, such as grasses, hard-woods, and soft-woods, Chinese quince fruits are more likely to be generally accepted by consumers as a source of natural antioxidants because of its edibility and historical medical application. Qin et al. [18] reported the lignin structure of Chinese quince fruits after enzymatic pretreatment and their application in antioxidant. However, knowledge of high yield Chinese quince fruits lignin is still limited; in particular, the knowledge needed for industrial use of quince fruits lignin with high antioxidant properties is limited. Therefore, additional investigations of the pretreatment for lignin separation of the Chinese quince fruits are still needed. Analyzing and describing these investigations will facilitate the utilization of Chinese quince fruits, especially as a potential source of natural antioxidants for the food industry.

In the present work, Chinese quince fruits were subjected to the AEOP process. Three factors that influence lignin yield, structure, and antioxidant activity were assessed, namely: pretreatment temperatures (140, 160, 180, 200, 220, and 240 °C), times (30, 60, 90, 120, and 150 min), and ethanol concentrations (40%, 50%, 60%, 70%, and 80%). Structural characteristics and antioxidant activities of auto-catalyzed ethanol organosolv lignin (AEOL) samples were investigated. Additionally, the carbohydrate composition and morphological of the solid residues after the AEOP process were detected by HPAEC and scanning electron microscopy (SEM), respectively.

2. Materials and methods

2.1. Materials

Fresh Chinese quince fruits (*Chaenomeles sinensis*) were obtained from a local orchard in Huiji district (Zhengzhou, China). The fruits were sliced into layers about 5 mm thick and oven-dried at the temperature of 60 °C for 48 h. Dried slices were pulverized with a pulverizer to obtain 40–60 mesh powder. Subsequently, the 40–60 mesh powder was stored in a desiccator before use. All chemical reagents used in the present work were analytical grade.

2.2. Preparation of lignin samples

The 40–60 mesh powder was dewaxed with a toluene-ethanol (2:1, v/v) mixture at around 90 °C for 8 h in a Soxhlet apparatus. Soxhlet extraction would remove soluble phenolics which could interfere with the subsequent structural and antioxidant activity analysis of lignin samples. Subsequently, the dewaxed powder was air-dried and stored in a desiccator before use. The dewaxed powder was 78.5% in relation to the dry-weight of initial quince fruits. The moisture content of the dewaxed powder was 2.10 ± 0.06%.

The treatment of dewaxed Chinese quince fruits powder was performed in a 500 mL stainless steel cylindrical reactor (Century Senlang experimental apparatus Co., Ltd., Beijing, China). A series of experiments were conducted at 140–240 °C reaction temperature, 30–150 min reaction time, and 40–80% ethanol concentrations. 20 g of dewaxed powder were loaded in the reactor equipped with an internal magnetic stirrer, and mixed with 200 mL of water-ethanol solution. The reactor was tightly sealed and heated to the desired reaction temperature for the desired time with the stirring rate of 500 rpm/min, after which the reactor was cooled to 60 °C through water circulation. Then, the pulp was filtered with filter paper to separate the liquid and residual solid. The residual solid was washed using 60 mL warm (60 °C) aqueous ethanol with the same concentration as used in the AEOP process. The filtrate and washing solutions were combined and concentrated to 40 mL using a rotary evaporator, then poured into 10-fold volume distilled water to precipitate the lignin. The precipitated lignin was separated by filtration with filter paper. After washing with acidic water (pH = 2.0) three times and freeze-drying, lignin was obtained and labeled as AEOL. The residual solids were oven-dried and labeled as RS. The yields of AEOL samples and residual solids were calculated as the percentage of the dewaxed powder (dried weight). An overview of the auto-catalyzed ethanol organosolv experiments performed is showed in Table 1. All extraction experiments were replicated three times.

2.3. Characterization of residual solids

The monosaccharide composition of residual solids was measured by HPAEC [19]. Briefly, RS samples (4–6 mg) were firstly hydrolyzed with sulfuric acid (72%) for 45 min at 25 °C. Then the sulfuric acid was diluted to 3% followed by hydrolysis at 105 °C for 2.5 h. Then the mixtures were diluted 50-fold and the filtrates were analyzed by an HPAEC system (Dionex ISC3000, Sunnyvale, CA, USA) with an amperometric detector, a guard PA-20 column (3 × 30 mm, Dionex) and a CarbopacTMPA-20 column (4 × 250 mm, Dionex).

The lignin content of dewaxed Chinese quince fruits powder and RS samples were determined according to the NREL standard process [20].

The changes in the surface microstructure of dewaxed powders and residual solids treated at different temperatures were observed by SEM (HT-7700, Hitachi, Japan), operated at an accelerating voltage of 3 kV. Prior to imaging, residual solid samples were sputter-coated with a layer of gold using an EICO IB-5 sputter coater.

2.4. Characterization of lignin

The FT-IR spectra of AEOL samples were obtained using a Nicolet-510 FT-IR spectrophotometer (Thermo Fisher, Lexington, MA, USA). Lignin samples were ground with KBr powder, and then pressed into 1 mm sheets. Sixty-four scans were recorded for each sample in the frequency of 4000–400 cm^{-1}.

The molecular weights (M_w and M_n) of AEOL samples were estimated on an Agilent 1200 system (Agilent Technologies, USA) equipped with an ultraviolet detector (UV) at 240 nm on a PL-gel 10 mm MixedB 7.5 mm ID column calibrated with different molecular weight monodispersed polystyrene standards (M_w in the range of 500–1,000,000). Lignin samples were acetylated prior to GPC analyses. Briefly, 100 mg lignin was dissolved in 4 mL acetic anhydride/pyridine (1:1, v/v) and reacted at 25 °C for 24 h in darkness. Then, the product was precipitated with acidic water (pH = 2.0), passed through filter paper, and freeze-dried [21]. The acetylated AEOL samples were dissolved in tetrahydrofuran (1 mg/mL), and a 10 μL aliquot of solution was injected into the GPC.

The thermal properties of AEOL samples were studied by thermogravimetric (TG) and differential thermogravimetric (DTG) using a TGA Q500 system (TA instrument, USA). Approximately 10 mg of lignin sample was heated from 45 °C to 800 °C at the rate of 10 °C/min in a nitrogen atmosphere.

Analytical pyrolysis was performed with a pyrolyzer (EGA 3030, Shimadzu, Japan) connected to a gas chromatograph-mass selective detector (Agilent 7890B-5977B, Agilent Technologies Inc., USA). The pyrolysis of lignin samples (500 μg) were performed at 500 °C for 20 s. The released volatile products were separated on a capillary column (DB-5MS, 30 m × 0.25 mm × 0.25 μm). The GC oven temperature was programmed to increase from 50 °C (4 min) to 100 °C at 20 °C/min and then to 280 °C (5 min) at 6 °C/min. The identification of pyrolysis products was made based on the NIST17 and Wiley libraries. Peak molar areas were determined for each sample pyrolysis product; the summed molar areas were expressed as percentages.

Table 1
The overview of the auto-catalyzed ethanol organosolv pretreatment experiments performed and antioxidant activities of AEOL samples.

Series	Experiments	Pretreatment conditions			Antioxidant activities		
		Temp. (°C)	time (min)	EtOH (%)	DPPH (IC_{50}, μg/mL)	ABTS (IC_{50}, μg/mL)	FRAP (mmol of $FeSO_4$/g of AEOL)
Experiments of different temperatures	1[a]	140	90	60	78.0 ± 3.6^{a}	24.3 ± 1.0^{bc}	3.4 ± 0.08^{b}
	2	160	90	60	89.2 ± 2.0^{ac}	27.2 ± 2.1^{def}	3.1 ± 0.10^{def}
	3	180	90	60	106.9 ± 2.7^{e}	35.9 ± 0.7^{hi}	2.8 ± 0.09^{h}
	4	200	90	60	108.2 ± 2.0^{e}	37.1 ± 1.2^{ig}	2.6 ± 0.08^{i}
	5	220	90	60	109.4 ± 2.8^{ef}	41.1 ± 1.5^{l}	2.7 ± 0.06^{h}
	6	240	90	60	114.3 ± 3.0^{fg}	39.8 ± 1.1^{kl}	2.2 ± 0.05^{k}
Experiments of different times at 160 °C	7	160	30	60	88.5 ± 2.2^{c}	29.1 ± 0.8^{f}	3.2 ± 0.04^{de}
	8	160	60	60	88.8 ± 2.8^{c}	25.1 ± 1.1^{bcd}	3.3 ± 0.07^{cd}
	2	160	90	60	89.2 ± 2.0^{ac}	27.2 ± 2.1^{def}	3.1 ± 0.10^{def}
	9	160	120	60	87.8 ± 1.1^{c}	26.2 ± 0.4^{cde}	3.1 ± 0.07^{ef}
	10	160	150	60	89.1 ± 2.0^{c}	25.8 ± 1.2^{cd}	3.1 ± 0.06^{def}
Experiments of different times at 200 °C	11	200	30	60	99.7 ± 3.3^{d}	45.4 ± 1.8^{m}	2.4 ± 0.09^{j}
	12	200	60	60	101.1 ± 2.5^{d}	34.2 ± 1.3^{gh}	3.0 ± 0.07^{fg}
	4	200	90	60	108.2 ± 2.0^{e}	37.1 ± 1.2^{ig}	2.6 ± 0.08^{i}
	13	200	120	60	106.2 ± 2.7^{e}	38.3 ± 1.0^{gk}	2.7 ± 0.05^{hi}
	14	200	150	60	101.2 ± 1.7^{d}	33.1 ± 0.9^{g}	3.0 ± 0.03^{fg}
Experiments of different times at 240 °C	15	240	30	60	119.2 ± 4.6^{g}	44.1 ± 1.2^{m}	2.7 ± 0.04^{h}
	16	240	60	60	114.4 ± 1.4^{fg}	34.2 ± 1.2^{gh}	3.0 ± 0.02^{g}
	6	240	90	60	114.3 ± 3.0^{fg}	39.8 ± 1.1^{kl}	2.2 ± 0.05^{k}
	17	240	120	60	113.9 ± 3.0^{f}	39.1 ± 0.8^{gkl}	2.9 ± 0.02^{g}
	18	240	150	60	111.3 ± 2.9^{ef}	37.9 ± 1.1^{igk}	2.8 ± 0.03^{h}
Experiments of different EtOH	19	160	90	40	84.3 ± 2.8^{bc}	29.3 ± 0.6^{f}	3.1 ± 0.04^{efg}
	20	160	90	50	85.3 ± 3.0^{bc}	28.3 ± 0.9^{ef}	3.4 ± 0.05^{bc}
	2	160	90	60	89.2 ± 2.0^{ac}	27.2 ± 2.1^{def}	3.1 ± 0.10^{def}
	21	160	90	70	81.1 ± 1.7^{b}	25.1 ± 0.7^{bcd}	3.2 ± 0.07^{de}
	22	160	90	80	82.1 ± 1.7^{ab}	23.2 ± 1.0^{b}	2.9 ± 0.09^{g}
	BHT[b]	–	–	–	131.1 ± 3.7^{h}	20.5 ± 0.5^{a}	3.6 ± 0.10^{a}

The data of antioxidant activities were reported as mean ± SD. Means with different lowercase letters in a column are significantly different ($p < 0.05$) by the Duncan's test.
[a] Lignin sample obtained by experiment 1 was labeled as AEOL-1, and so on.
[b] BHT, butylated hydroxytoluene.

The NMR spectra of AEOL samples were acquired using a Bruker Avance III HD 500 MHz spectrometer. For the 2D-HSQC NMR experiments, 50 mg of AEOL samples were dissolved in 500 μL DMSO-d_6. The acquisition parameters were as detailed in a previous paper [22]. For the ^{31}P NMR spectra, 40 mg of lignin sample was dissolved in 500 μL $CDCl_3$/anhydrous pyridine (1:1.6, v/v, solvent A). 100 μL internal standard solution of cyclohexanol (10.85 mg/mL, in solvent A) and 100 μL relaxation reagent of chromium (III) acetylacetonate (5 mg/mL, in solvent A) were then added. Finally, 100 μL derivatization reagent (2-chloro-4,4,5,5-tetramethyl-1,3,2-dioxaphopholane) was added. The reaction solution was kept for 15 min before subsequent NMR analysis.

2.5. Determination of antioxidant performance

2.5.1. DPPH free radical scavenging assay

The activities of AEOL samples in scavenging DPPH (2,2-diphenyl-1-picrylhydrazyl) free radicals were measured according to a published method [23] with some modifications. 10 μL AEOL samples in dioxane/water (90:10, v/v) with seven concentrations from 0.05 to 1.0 mg/mL were mixed with 190 μL of 24 μg/mL DPPH-methanol solution. After reaction at 25 °C for 20 min in the dark, the absorbance of the mixture was measured at 520 nm by a Multiskan FC (Thermo Fisher). Each DPPH assay was carried out in triplicate, and commercial antioxidant BHT was used as a reference. The DPPH free radical scavenging activities (RSA) of AEOL samples were calculated according to Eq. (1)

$$RSA\ (\%) = \left(\frac{A_0 - A_1}{A_0}\right) \times 100\% \quad (1)$$

A_0: $A_{520\ nm}$ of the blank sample; A_1: $A_{520\ nm}$ of DPPH solution. The IC_{50} values (half maximal inhibitory concentration) were further calculated according to the RSA (%) under different sample concentrations.

2.5.2. Scavenging of ABTS radical

The ABTS assay was performed based on the method of Baltrušaitytė et al. [24] with some modifications. ABTS•$^{+}$ was generated by mixing 50 mL of ABTS stock solution (2 mM ABTS in 50 mM phosphate buffered saline, pH = 7.4) with 0.5 mL of $K_2S_2O_8$ water solution (70 mM). The mixture was kept for 12–16 h at 25 °C in the dark. Before being used, the ABTS•$^{+}$ solution was diluted with phosphate buffered saline to get an absorbance of 0.700 ± 0.003 at 734 nm. Then 0.15 mL of each sample in dioxane/water (90:10, v/v) with seven concentrations from 0.01 to 0.1 mg/mL were added to 2.85 mL of the ABTS• $^{+}$ solution. Absorbance of the mixture was measured at 734 nm after 15 min. The ABTS•$^{+}$ radical scavenging activity (RSA) of AEOL samples were calculated according to Eq. (2)

$$RSA\ (\%) = \left(\frac{A_0 - A_1}{A_0}\right) \times 100\% \quad (2)$$

A_0: $A_{734\ nm}$ of the blank sample; A_1: $A_{734\ nm}$ of ABTS•$^{+}$solution. The IC_{50} values (half maximal inhibitory concentration) were further calculated according to the RSA (%) under different sample concentrations.

2.5.3. Ferric reducing antioxidant power assay (FRAP)

The FRAP assay was done utilizing the method reported by Vázquez et al. [25] with slight modifications. The working FRAP reagent was freshly prepared by mixing 1 volume of TPTZ (10 mM) in HCl (40 mM) with 1 volume of $FeCl_3 \cdot 6\ H_2O$ (20 mM) in deionized water and with 10 volumes of acetate buffer (300 mM, pH = 3.6). Before being used, the freshly prepared FRAP reagent was warmed to 37 °C. 0.15 mL of each lignin sample (0.1 mg/mL) in dioxane/water (90:10, v/v) was added to 2.85 mL of the FRAP reagent. After a 30 min incubation at 37 °C, the absorbance of the reaction solution was measured at 593 nm. Standard solutions of $FeSO_4 \cdot 7H_2O$ (25–800 μM, dissolved in deionized water) were prepared to plot a calibration curve (y = 0.9536x-0.0686, R^2 = 0.9959). The commercial antioxidant BHT served as a reference.

The experiments were carried out in triplicate and the results were expressed as mM $FeSO_4 \cdot 7H_2O$ per g lignin sample.

2.6. Statistical analysis

All experiments were replicated three times, and evaluated by analyses of variance (ANOVA) using SPSS version 19 package (IBM, Armonk, NY). A Duncan's test was performed to determine significant differences between means ($p < 0.05$).

3. Results and discussion

3.1. Yield and monosaccharide compositions of AEOL samples and residue solids

During the AEOP process, the severe temperatures and pressure conditions led to the release of acetic acid by hydrolysis of acetyl side groups of the hemicellulose. Then, this acetic acid decreased the pH of the organosolv liquor, and strengthened the delignification and hemicellulose hydrolysis [26]. As can be seen from Fig. 1, temperature and ethanol concentrations were the most significant factors to affect AEOL yield. The maximum lignin yield was observed from the pretreatment conditions of 200 °C, 90 min, and 60% aqueous ethanol (14.40%, experiment 4). Wildschut et al. [26] reported a similar observation of ethanol-based organosolv pretreatment of wheat straw. In that work, the maximum lignin yield (14.7%) was observed from the pretreatment conditions of 210 °C, 90 min, and 50% aqueous ethanol when the catalyzer was absent. The combination of lignin depolymerization and dissolution of degraded lignin fragments offered the possibility to separate lignin during the pretreatment process [9]. During the AEOP process, with the increase of temperature, the delignification was promoted and thus the dissolution of lignin was enhanced [27]. Therefore, the increased temperature led to the increased yields of AEOL samples and the decreased lignin content of residual solids (Table 3). However, a further increase in temperature beyond 200 °C resulted in decreased lignin yields. This could be explained by the excessive depolymerization of lignin molecules and the formation of highly soluble small fragments at high temperatures. These fragments were still soluble in a low ethanol concentration and could not be recovered by the precipitation step [9], leading to a decrease of lignin yield. Furthermore, the soluble lignin could condense in auto-catalyzed organosolv pretreatment at higher temperatures, leading to more condensed lignin in the residual fractions and increased lignin content in the residual solids (RS-5 and RS-6, Table 3) [28].

The maximum lignin yield (13.20%) occurred at 50% aqueous ethanol (Experiment 20). That means the lignin yields decreased with increasing ethanol concentration (Experiment 2, 21, 22). This can be explained by the depressed delignification at higher pH (or lower hydrogen ion concentration) and the poor solubility of lignin at the unsuitable ethanol concentrations. The lower pH expedited the cleavage of α- and β- ether linkages in lignin and the bonds within lignocellulose complex, resulting in an enhancement of the delignification process [9]. Wildschut et al. [26] explored wheat straw biorefining by ethanol organosolv, and found that the pH of the organosolv liquor increased from 4.9 to 5.7 when the ethanol concentration was increased from 50% to 80%. According to the literature, the change of the dissociation constant of organic acids in the organosolv liquor was probably responsible for the pH increase with the acetone proportion. Furthermore, Ni and Hu [29] reported that the maximum solubility of the ALCELL lignin was at an ethanol concentration of about 70%. Overall, the optimum organosolv concentration for the organosolv pretreatment was an equilibrium between organosolv liquor pH needed for the acid-catalyzed process and the solubility of lignin [26]. From this study, the most effective ethanol concentration for the extraction of AEOL was shown to be 50%.

The polysaccharides covalently linked to the lignin in the Chinese quince fruits were mainly responsible for the carbohydrates present in

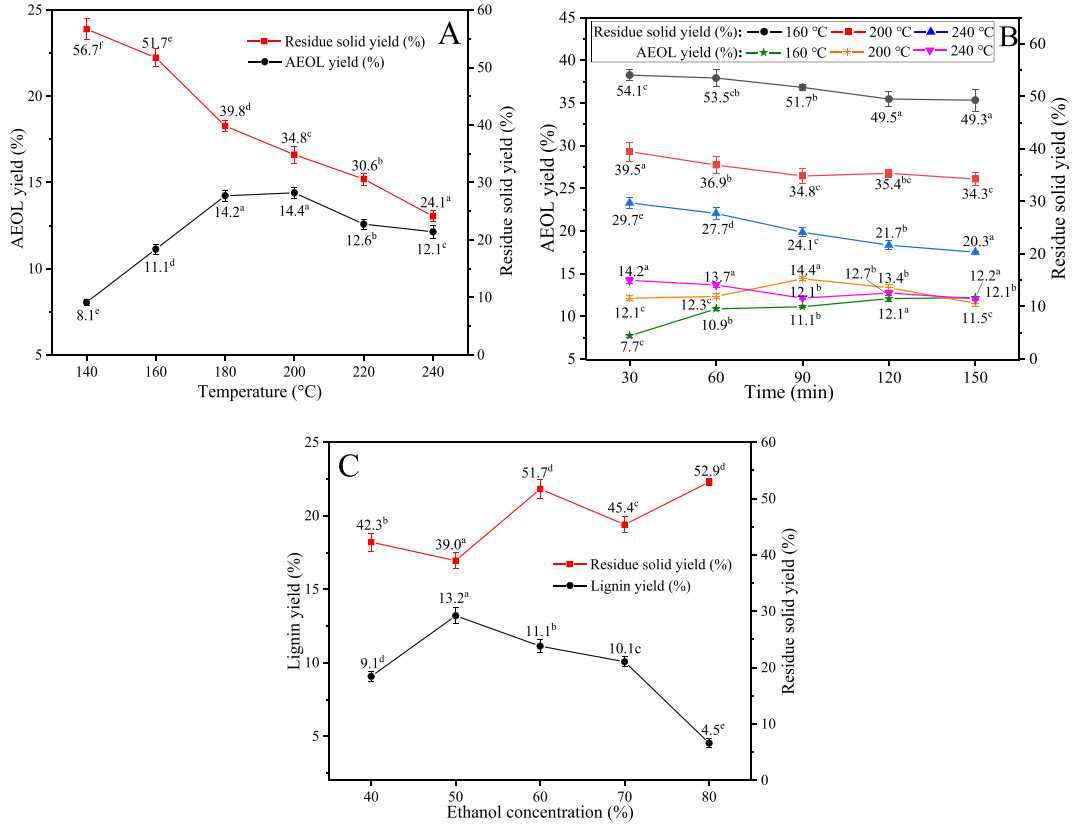

Fig. 1. Lignin yield and residue solid yield during auto-catalyzed ethanol organosolv pretreatment for Chinese quince fruits. (A) 90 min, 60% ethanol concentration, and temperatures from 140 to 240 °C; (B) Temperatures (160 °C, 200 °C, and 240 °C), 60% ethanol concentration, and time from 30 to 150 min; (C) 90 min, 160 °C, and ethanol concentration from 40 to 80%.

AEOL samples [30]. As can be seen in Table 2, the total sugar content decreased as pretreatment temperature rose, and reached the minimum content of 0.78% (AEOL-6) at 240 °C. One of the important reasons for this phenomenon was the intensified decomposition of lignin-carbohydrate complexes (LCC) as the temperature increased. Xylose was the major sugar component in the lignin samples (AEOL-3, AEOL-4, AEOL-5, and AEOL-6), comprising 69.23–77.04% of total sugar, but the amounts of arabinose, galacturonic acid, and glucuronic acid were drastically reduced until undetectable. The results suggest that most sugar attached to lignin was removed at high pretreatment temperature, and only a small amount of sugar remained, most of which was xylose.

The lignin content of Chinese quince fruits was 21.00 ± 0.86% (w/w) as determined by the NREL standard process [20]. The sugar analyses revealed that xylose was the dominant constituent in Chinese quince fruits, while polgalacturonic acid and polglucuronic acid were only present in minor quantities. After pretreatment, the lignin content decreased significantly. The lowest value was RS-4 (9.44 ± 0.38%), indicating that the optimum temperature for delignification process ranged between 200 and 220 °C. For all the residual solids, the contents of arabinan, galactan, polgalacturonic acid, and polglucuronic acid were lower than those of the raw material. In addition, total sugar content decreased as the pretreatment temperature. This decrease may be due to the hydrolysis of hemicellulose during the pretreatment. Xylose, which originated from the hydrolysis of hemicellulose, could be further transformed into derivative chemicals such as furfural and acetic acid at high pretreatment temperatures. The decrease of xylan content in residual solids suggested that this transformation was enhanced by increasing temperature [31]. Moreover, the proportion of glucan (mainly from cellulose) increased from 12.63% to 46.91%. These results suggest that cellulose was partly retained in the residual solids, whereas most of the hemicellulose and lignin were removed, especially for the samples subjected to AEOP at higher temperatures, such as RS-5 and RS-6. As can be seen in the SEM images (Fig. S1), the number of cracks that appeared on the surface of residual solids extensively increased with the increasing pretreatment temperature, demonstrating that the cell wall as a physical barrier was effectively broken. The effective pretreatment could break the chemical linkages between lignin and hemicelluloses, breaking the integrity of the cell wall so that solvent could access its complex structural networks [32].

3.2. FT-IR analyses

FT-IR spectra were used to analyze the functional groups of AEOL samples. Figs. 2, S2, and S3 show the spectra of AEOL samples in terms of the pretreatment temperatures, times, and ethanol concentrations used, respectively. The spectral profiles in Fig. 2 show some differences except for the intensities of the absorption bands of vibration, suggesting that the structure of the six lignin samples changed due to difference in the pretreatment temperature. The spectral profiles in Figs. S2 and S3 exhibit very similar patterns, implying that the structure of AEOL samples did not significantly change under different pretreatment times and ethanol concentrations. The broad band at 3330 cm^{-1} is assigned to the O—H stretching vibration in aromatic and aliphatic OH

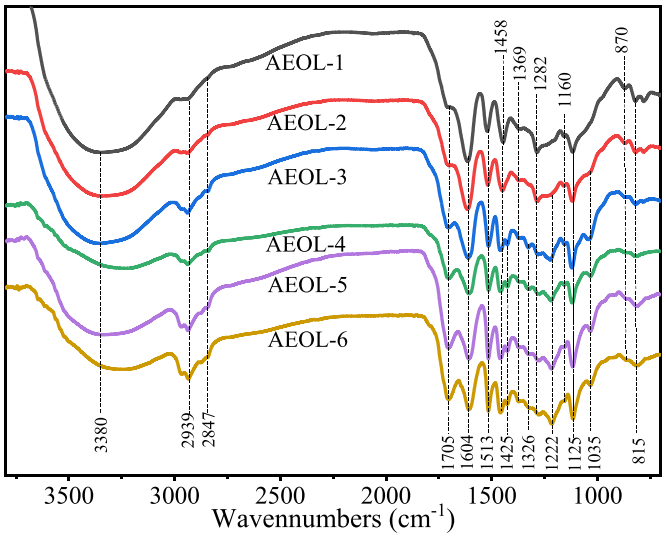

Fig. 2. FT-IR spectra of AEOL samples with respect to different pretreatment temperatures.

groups, whereas the absorption at 2939 cm^{-1} is assigned to the C—H symmetrical and asymmetrical vibrations of CH_2 and CH_3 groups [33]. In Fig. 2, the spectra of AEOL-1 and AEOL-2 exhibited weaker peaks at 1705 cm^{-1} than that of AEOL-5 and AEOL-6, indicating that the high temperature during the AEOP process may result in the cleavage of more β-O-4′ linkages, generating more carbonyl groups [26]. It was reported that the aliphatic hydroxyl and conjugated carbonyl group had a negative effect on the antioxidant activity of lignin [9,22]. Therefore, the higher concentrations of conjugated carbonyl groups in AEOL-5 and AEOL-6 were likely to result in lower antioxidant activity of these two samples (see data in Table 1). The signals at 1604, 1513, and 1425 cm^{-1} arise from the aromatic ring vibrations of the phenyl propane skeleton, and these signal patterns are typical of lignin [34]. The absorption bands at 1326 and 1222 cm^{-1} are most likely owing to syringyl rings breathing with C—O stretching, and the band at 1035 cm^{-1} is related to aromatic C—H in-plane deformation vibrations [33]. The typical absorption at 1125 cm^{-1} is an unmistakable band of a GS lignin, and the absorption band at 1160 cm^{-1} is assigned to antisymmetric C—O stretching of ester groups. The absorption at 1369 cm^{-1} is the typical C—H stretching of acetate methyl groups, suggesting that natural acetylation occurred in AEOL samples [14]. The peak at 1106 cm^{-1} corresponds to the C—H out-of-plane vibration of aromatic rings in the lignin samples [34].

3.3. Molecular weight distributions of lignin samples

Considering the pretreatment temperature was the most significant factor that affect the AEOP process, the AEOL-1 to AEOL-6 samples were selected to be thoroughly characterized. The number-average (M_n), weight-average (M_w), and the polydispersity index (PDI) of the six samples were determined by GPC. The data are given in Table 2, and the GPC curves are shown in Fig. 3. As the pretreatment temperatures increased

Table 2
Monosaccharide compositions and molecular weight of AEOL samples.

Lignin samples	Lignin content (%)	Total sugar (%)	Monosaccharide content (based on total sugar, %)[a]						M_w (g/mol)	M_n (g/mol)	M_w/M_n
			Glu	Xyl	Ara	Gla	Gal-A	Glu-A			
AEOL-1	82.02 ± 1.10	16.69	8.03	9.23	37.47	23.62	20.08	1.56	12,896	3887	3.32
AEOL-2	83.98 ± 0.98	14.61	4.86	40.96	43.08	8.29	2.26	0.55	11,870	3721	3.19
AEOL-3	88.60 ± 1.23	10.17	2.29	75.04	12.58	4.47	5.24	0.38	8614	2830	3.04
AEOL-4	95.12 ± 1.36	3.78	7.92	77.04	6.07	8.97	ND[b]	ND	5636	2255	2.50
AEOL-5	97.48 ± 0.84	1.50	14.67	75.33	ND	10.00	ND	ND	3528	1766	2.00
AEOL-6	98.52 ± 1.06	0.78	28.21	69.23	ND	2.56	ND	ND	2814	1567	1.80

[a] Glu, glucose; Xyl, xylose; Ara, arabinose; Gal, galactose; Gal-A, galacturonic acid; Glu-A, glucuronic acid.
[b] ND, not detected.

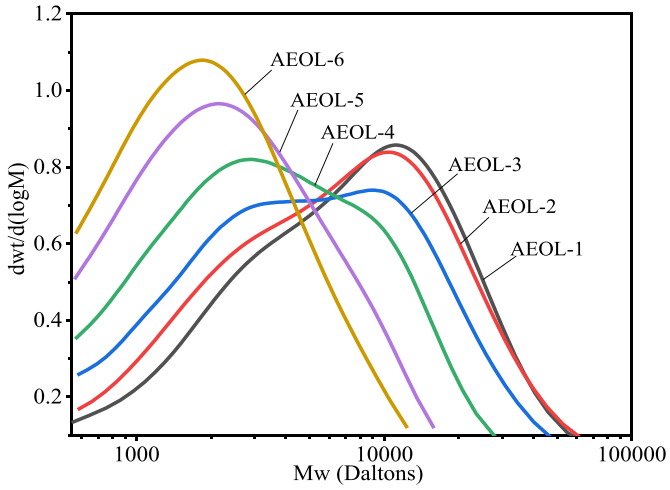

Fig. 3. Molecular weight distributions of AEOL samples with respect to different pretreatment temperatures.

from 140 to 240 °C, the values of M_w and M_n decreased from 12,896 g/mol to 2814 g/mol, and from 3887 g/mol to 1567 g/mol, respectively. Furthermore, the lignin samples extracted at lower temperatures showed much higher PDI values than those extracted at higher pretreatment temperatures. Overall, higher molecular weight fractions showed higher PDI. During the AEOP process, repolymerization and depolymerization of lignin are two competitive reaction processes and occurred simultaneously [14]. The decreased molecular weights and the improved homogeneity of AEOL inferred that depolymerization was the dominating reaction during the AEOP process. It means that the AEOL samples extracted at higher temperatures consist of more small lignin fragments whose molecular weight was relatively uniform. The higher molecular weight of the AEOL samples (AEOL-1, AEOL-2, and AEOL-3) also might be explained by their higher content of carbohydrates. A previous investigation documented that carbohydrate chains linked to lignin could increase the hydrodynamic volume of the lignin, thereby also increasing its apparent molecular weight in GPC studies [35].

3.4. Py-GC/MS analyses

Py-GC/MS analyses were utilized to explore the influence of pretreatment temperatures on the structure of AEOL samples. The technique is an efficient analytical method that can provide lignin pyrolysis product information. Table 4 summarizes the detected 39 lignin-degradation products and the relative proportions (%) of these products. The pyrolysis product proportions of the six lignin samples have significant differences, and the pyrolysis phenolic products originated from syringyl (S), guaiacyl (G), and *p*-hydroxyphenyl (H) units as well as from *p*-hydroxycinnamic acids. As the chart shows, the pyrolysis products were very complex and included phenols, ketones, acids, and aldehydes. Phenols were detected to be most abundant. Noticeably, the high amounts of 2-methoxy-4-vinylphenol (peak 14) may be due to the presence of ferulic acid or *p*-coumaric acid in lignin, since ferulic acid and *p*-coumaric acid will yield 2-methoxy-4-vinylphenol via decarboxylation degradation under pyrolytic conditions [18]. As it did not entirely arise from the pyrolysis of lignin, 2-methoxy-4-vinylphenol cannot be used for the calculation of S/G ratio upon Py-GC/MS.

As shown in Table 4, AEOL-1 and AEOL-2 showed lower S/G ratios (0.13 and 0.33, respectively), while AEOL-3, AEOL-4, AEOL-5, and AEOL-6 showed higher S/G ratios (1.46, 1.69 and 1.58 and 1.82, respectively). It was obvious that the proportions of pyrolysis products which originated from G units, such as 1,2-benzenediol (peaks 8, 9) and 4-methyl-1,2-benzenediol (peaks 15, 16), decreased as the pretreatment temperature increased. By contrast, proportions of pyrolysis products which originated from S units, such as 2,6-dimethoxyphenol (peak 17) and 1, 2, 3-trimethoxybenzene (peak 25), increased as temperature increased. The significant changes in the proportions of these pyrolysis products led to a wide range of S/G ratios. During AEOP, the degradation and condensation of lignin concurrently occurred [14]. The increased S/G ratios of the six lignin samples revealed that degradation took place preferentially at G-units as the pretreatment temperature increased. In addition, the condensation of lignin was enhanced with the increased pretreatment temperature (Fig. 4), implying that condensation also took place preferentially at G units.

3.5. Thermal analyses

The thermal properties of AEOL samples were investigated by TG analyses and DTG thermograms. The relationship between weight losses and temperatures (TG curves) are shown in Fig. 4A, while the corresponding rates of weight loss (DTG curves) are shown in Fig. 4B. As shown in Fig. 4A, the first weight loss stage (2–4%) from 45 to 200 °C revealed the evaporation of residual moisture in lignins and the emission of volatile substances such as carbon monoxide and carbon dioxide [18], while the weight losses from 200 to 500 °C represented the decomposition of the complex structures in lignin polymers. The cleavage of α- and β- aryl alkyl ether linkages happened at 150 to 300 °C, while the carboxylation or carbonylation of aliphatic hydroxyl groups and the dehydrogenation of side chains happened at 350–400 °C. The last step of weight loss (above 500 °C) was ascribed to the decomposition and condensation reactions of the aromatic skeleton (rings). At this stage, the cleaving of methoxyl groups (-OCH_3) in lignin occurred, which would lead to charring and the emission of CH_4 [36].

As shown in Fig. 4A, the char residues of these lignin samples were recorded in the range of 42.19–49.26%. The observations are consistent with the results previously reported for corncob hydrothermally pretreated EOL and wheat straw EOL [3,37]. An explanation for the

Table 3
Lignin content and carbohydrate composition of the Chinese quince fruits before and after the AEOP process.

Residue solids	Lignin content (%)	Carbohydrate content (%)					
		Glucan	Xylan	Arabinan	Galactan	Pgal-A[a]	Pglu-A[b]
RS[c]	21.00 ± 0.86	12.63	41.01	8.57	8.92	3.96	2.76
RS-1	12.71 ± 0.45	34.88	43.80	1.75	3.29	0.56	0.39
RS-2	12.05 ± 0.36	37.09	42.47	1.00	2.29	0.29	0.16
RS-3	10.99 ± 0.40	42.94	34.89	0.36	1.65	0.09	0.07
RS-4	9.44 ± 0.38	45.33	25.92	0.06	0.99	0.09	ND[d]
RS-5	10.24 ± 0.45	46.49	10.32	ND	0.21	0.10	ND
RS-6	10.70 ± 0.41	46.91	2.27	ND	ND	0.11	ND

[a] Pgal-A, Polgalacturonic acid.
[b] Pglu-A, Polglucuronic acid.
[c] RS, dewaxed Chinese quince fruits powder without AEOP process. RS-1, RS-2, RS-3, RS-4, RS-5, and RS-6, the residue solids of dewaxed Chinese quince fruits powder after AEOP process at 140 °C, 160 °C, 180 °C, 200 °C, 220 °C, and 240 °C, respectively.
[d] ND, not detected.

Table 4
Identification and relative abundance (%) of the lignin-derived compounds from the Py-GC/MS of AEOL samples.

No.	Compound	Origin	AEOL-1	AEOL-2	AEOL-3	AEOL-4	AEOL-5	AEOL-6
1	Phenol	H	2.57	2.48	0.17	0.07	0.04	0.03
2	2-methylphenol	H	0.36	0.95	ND	ND	ND	ND
3	2-methoxyphenol	G	1.17	1.04	4.38	4.70	6.06	5.97
4	4-methylphenol	H	4.15	3.83	ND	ND	ND	ND
5	2,3-dimethylphenol	H	ND	0.80	0.36	ND	ND	0.63
6	2-methoxy-6-methylphenol	G	ND	0.09	0.20	ND	ND	ND
7	2-methoxy-4-methylphenol	G	2.31	4.19	5.29	6.57	6.67	7.67
8	1,2-benzenediol	G	39.32	30.26	7.89	5.15	3.65	4.01
9	1,2-benzenediol	G	7.49	4.16	2.95	2.15	1.35	1.30
10	3-methoxy-1,2-benzenediol	S	ND	4.93	ND	ND	ND	ND
11	3-methyl-1,2-benzenediol	G	ND	3.40	ND	ND	ND	ND
12	4-ethyl-2-methoxyphenol	G	3.55	ND	2.67	3.25	3.98	4.61
13	3-methoxy-1,2-benzenediol	S	ND	ND	4.98	5.13	5.60	6.16
14	2-methoxy-4-vinylphenol	G	4.74	4.87	7.38	4.79	3.42	3.28
15	4-methyl-1,2-benzenediol	G	15.59	12.95	0.80	1.83	ND	ND
16	4-methyl-1,2-benzenediol	G	3.88	1.96	2.18	0.93	ND	ND
17	2,6-dimethoxyphenol	S	6.56	ND	ND	13.49	17.65	19.11
18	2-methoxy-4-propylphenol	G	ND	ND	ND	1.20	1.45	1.93
19	2,6-dimethoxyphenol	S	ND	4.85	12.18	ND	2.48	3.19
20	3,4-dimethoxyphenol	S	ND	2.40	2.31	2.99	ND	ND
21	2,3-dihydroxybenzaldehyde	G	ND	0.73	ND	ND	ND	ND
22	Eugenol	G	ND	0.33	0.24	0.29	0.30	0.31
23	4-ethyl-1,3-benzenediol	G	0.08	ND	ND	ND	ND	ND
24	4-ethyl-1,2-benzenediol	G	ND	2.75	ND	ND	ND	ND
25	1,2,3-trimethoxybenzene	S	2.35	3.89	15.70	17.97	18.90	21.33
26	1-(3-hydroxy-4-methoxyphenyl)-ethanone	G	ND	ND	0.46	ND	0.45	ND
27	1-(2,6-dihydroxy-4-methoxyphenyl)-ethanone	G	ND	ND	4.45	ND	6.63	6.82
28	1-(4-hydroxy-3-methoxyphenyl)-2-propanone	G	ND	ND	ND	ND	ND	0.69
29	2,4,6-trihydroxyacetophenone	S	ND	1.01	ND	0.22	ND	ND
30	2,4,6-trihydroxyacetophenone	S	1.09	ND	ND	ND	ND	ND
31	Acetovanillone	G	ND	0.30	ND	ND	ND	ND
32	1-(4-hydroxy-3-methoxyphenyl)-2-propanone	G	ND	ND	0.47	ND	ND	ND
33	2,5-bis(1,1-dimethylethyl)-phenol	H	ND	0.07	ND	ND	ND	ND
34	5-tert-butyl-1,2,3-trihydroxybenzene	S	ND	1.41	ND	5.53	ND	ND
35	Homovanillyl alcohol	G	ND	ND	ND	0.58	ND	ND
36	1-(4-hydroxy-3-methoxyphenyl)-2-propanone	G	3.45	3.39	11.30	8.70	6.86	ND
37	2,6-dimethoxy-4-(2-propen-1-yl)-phenol	S	0.16	0.44	1.33	1.51	1.58	1.77
38	2,6-dimethoxy-4-(2-propen-1-yl)-phenol	S	ND	0.50	0.95	1.12	1.20	1.19
39	4-methoxyphenylglycolic acid	G	ND	ND	0.35	ND	ND	ND
40	3,5-dimethoxy-4-hydroxybenzaldehyde	S	ND	ND	1.51	1.79	1.64	1.59
41	2,6-dimethoxy-4-(2-propen-1-yl)-phenol	S	ND	ND	6.27	6.89	ND	ND
42	3-hydroxy-4-methoxycinnamic acid	G	0.88	ND	ND	ND	ND	ND
43	2,6-dimethoxy-4-(2-propen-1-yl)-phenol	S	ND	1.19	ND	ND	7.09	6.53
44	1-(4-hydroxy-3,5-dimethoxyphenyl)-ethanone	S	0.32	0.42	1.42	1.36	1.23	0.93
45	Homovanillyl alcohol	G	ND	ND	ND	ND	ND	0.94
46	4-hydroxy-3,5-dimethoxy-benzeneacetic acid	S	ND	0.40	ND	ND	ND	ND
47	2,4,6-trihydroxy-3-methylbutyrophenone	S	ND	ND	1.79	1.79	1.79	ND
		H%	7.08	8.13	0.53	0.07	0.04	0.03
		S%	10.47	21.44	54.58	59.72	59.11	62.43
		G%	82.45	70.43	44.89	40.21	40.85	37.54
		S/G	0.13	0.33	1.46	1.69	1.58	1.82

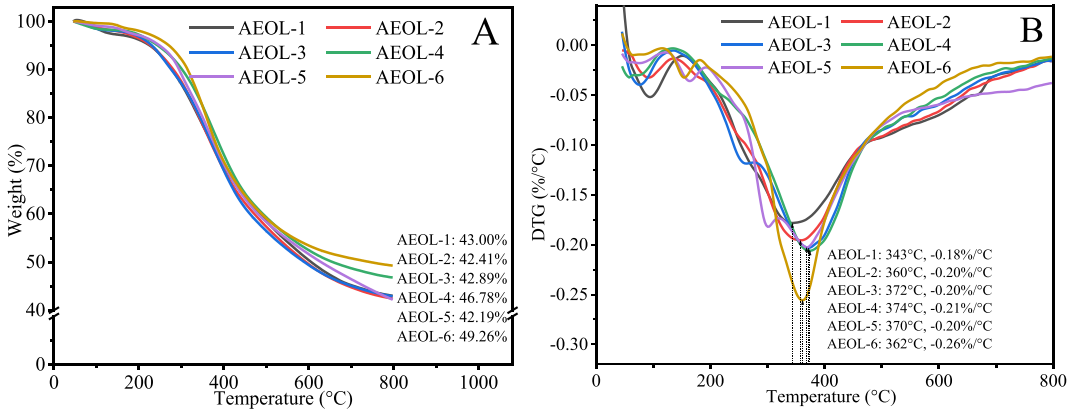

Fig. 4. TG curves (A) and DTG (B) curves of AEOL samples. A: The final solid residue yields are displayed. B: The maximum decomposition rates and the corresponding maximum decomposition temperatures are displayed.

lower residue yield of AEOL-1, AEOL-2, and AEOL-3 is the higher content of carbohydrate impurities. Under thermal degradation conditions, the cleavage of lignin-carbohydrate linkages releases part of the carbohydrate, which is much more easily pyrolyzed than lignin [30]. Furthermore, it was found that the char residues were 46.78% for AEOL-4 and 49.26% for AEOL-6. The higher char residues suggested that more stable lignin structures, such as condensed lignin, existed in AEOL-4 and AEOL-6, as confirmed by the analyses of 2D-HSQC NMR. Interestingly, although the AEOL-5 sample was extracted at 220 °C during the AEOP process, it had the lowest char residues of 42.19%. This was probably due to more methoxy groups (-OCH_3) and aryl alkyl ether linkages in that sample [36]. As can be seen in Fig. 4B, the first peak of the DTG curve for AEOL-5 was located at 298 °C; this peak represented the decomposition of the weaker β-O-4′ linkage during the lignin decomposition. The maximum degradation rates (DTG_{max}) of AEOL-1 appeared at the lowest temperature of all the AEOL samples, suggesting the lowest thermal stability of AEOL-1. This conclusion is supported by the fact that AEOL-1 had the highest content of carbohydrate.

3.6. NMR spectra analyses

3.6.1. 2D-NMR spectra analyses

2D-HSQC NMR was used to determine detailed structural features of the whole lignin macromolecule. AEOL-2, AEOL-4 and AEOL-6 were studied by 2D-HSQC NMR, and the C—H correlation signals were assigned according to previous papers [13,38,39]. The spectra of the three lignin samples in the side-chain region (δ_C/δ_H 50–90/2.5–6.0 ppm) and aromatic region (δ_C/δ_H 90–140/5.5–8.0 ppm) are shown in Fig. 5. The identified substructures are exhibited in Fig. 6.

The signals at δ_C/δ_H 63.5/3.34 ppm, ascribed to the methylene in α-ethoxylated β-O-4′ linkage (A'), were observed in the spectra of the three lignin samples, indicating the occurrence of α-ethoxylation during the AEOP process. It has been reported that α-ethoxylated β-O-4′ linkages (A') are formed easily during the AEOP process because of the substitution of hydroxyl group in α-position of lignin by ethanol [40]. As seen in Fig. 5, the signals for all the observed linkages were reduced as the pretreatment temperature increased, indicating that many linkages were cleaved at higher temperatures. As a result of the cleavages

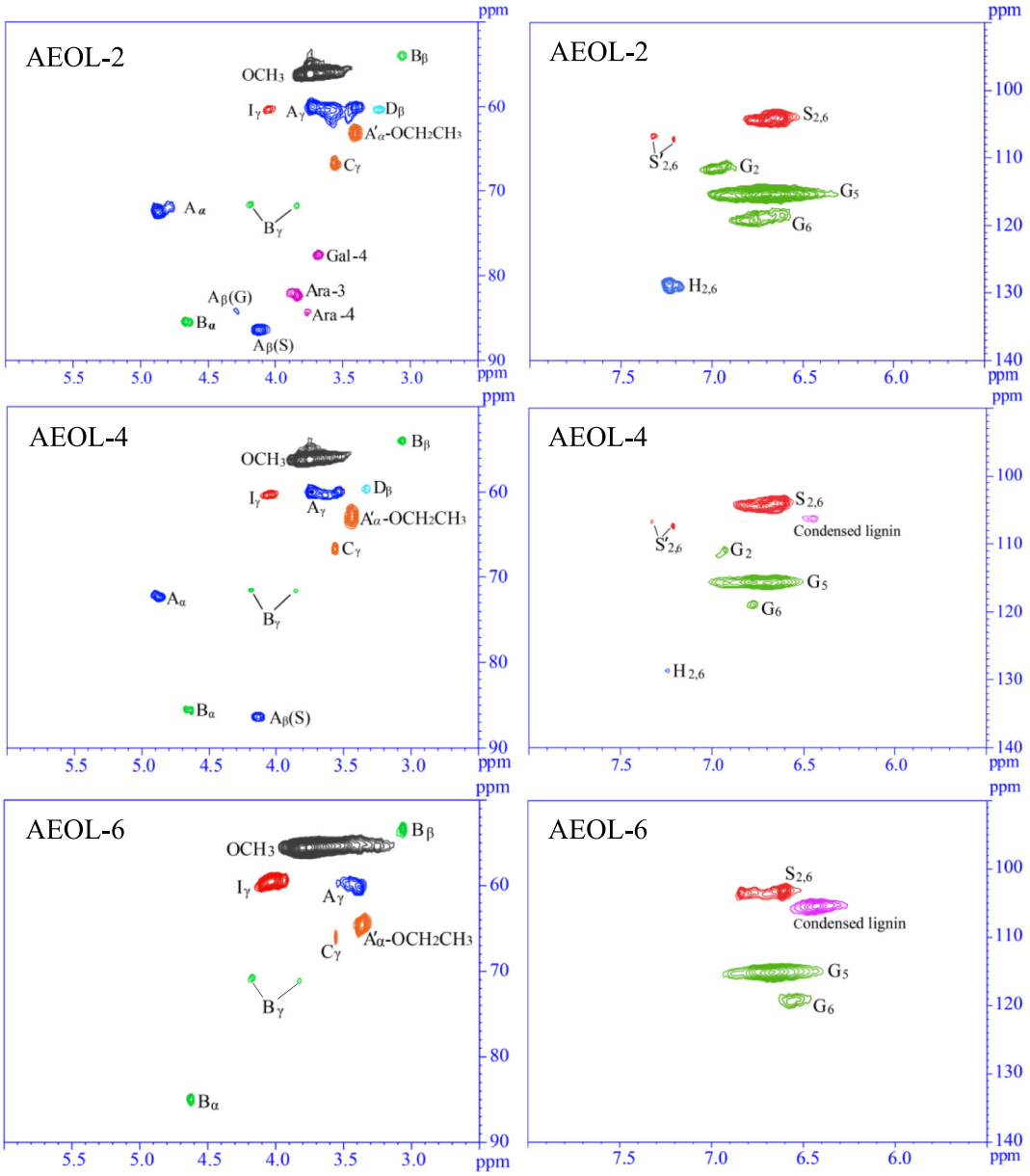

Fig. 5. 2D-HSQC-NMR spectra of AEOL samples.

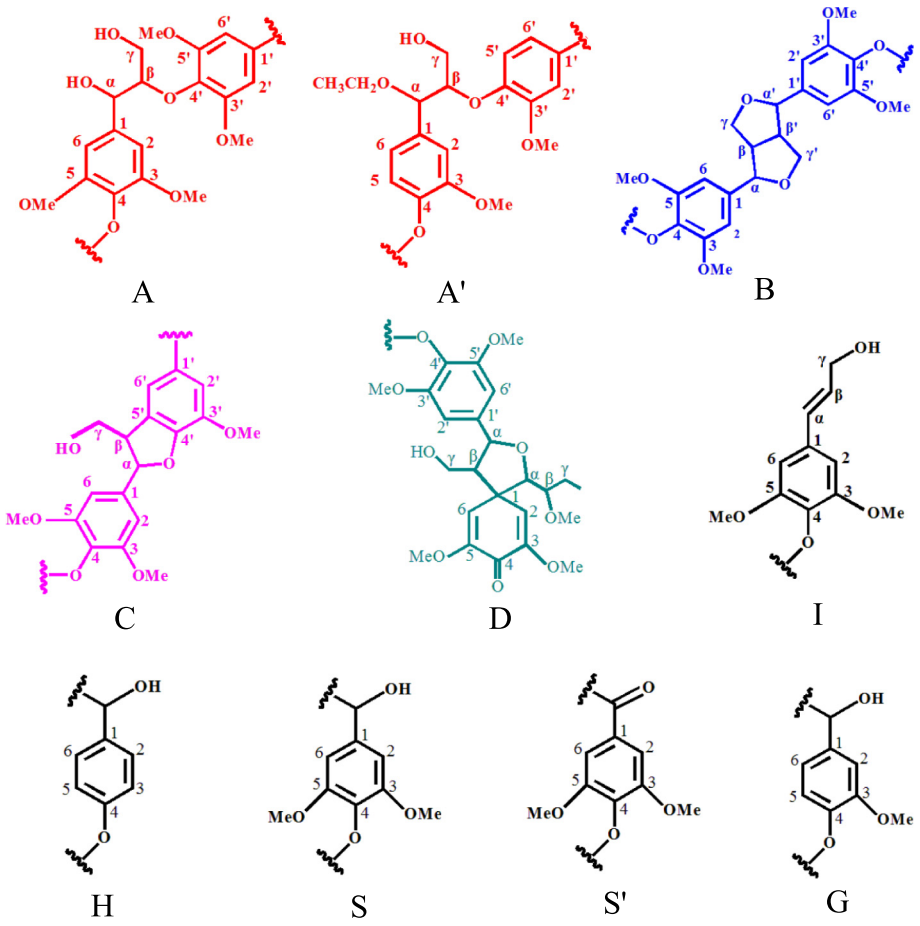

Fig. 6. Main lignin substructures in AEOL isolated from Chinese quince fruits after AEOP process. (A) β-O-4′ linkage; (A′) C_α-ethoxylation-β-O-4′ linkage; (B) resinol substructures formed by β-β′ linkage; (C) phenylcoumaran substructures formed by β-5′ linkage; (D) spirodienone substructure formed by β-1′ linkage; (G) guaiacyl unit; (H) *p*-hydroxyphenyl unit; (I) cinnamyl alcohol end-groups; (S) syringyl unit; (S′) oxidized syringyl units linked a carbonyl at C_α.

of lignin inter-unit linkages (mainly β-O-4′ linkage), the lignin molecular weights of AEOL samples decreased with increasing pretreatment temperatures, corresponding to the analyses by GPC. It is noteworthy to mention that the signals of carbohydrate impurities in AEOL-2 were also detected in the HSQC spectrum. The signals from galactose were present in the spectrum of AEOL-2 with C_4-H_4 correlations at δ_C/δ_H 77.7/3.62 ppm and the signals from C—H correlations at 3 and 4 positions in arabinosyl units appeared at δ_C/δ_H 84.31/3.74, 82.44/3.83 and 80.71/3.99 ppm, respectively. This was consistent with the result of sugar analyses (Table 2) that AEOL-2 had more carbohydrate impurities covalently linked to the lignin than AEOL-4 and AEOL-6.

In the aromatic region of the spectra of the three lignin samples, S, G, and H units were easily identified. The signals at δ_C/δ_H 112.0/6.93, 115.6/6.64 and 119.4/6.70 ppm, were ascribed to the C_2-H_2, C_5-H_5 and C_6-H_6 of G units, respectively, while the ones at around δ_C/δ_H 104.4/6.60 and 128.8/7.17 ppm were attributed to $C_{2,6}$–$H_{2,6}$ in S units and H units (not shown in the HSQC spectrum of AEOL-6). Additionally, fewer C_α-oxidized (C_α = O) structures of S-type unit ($S'_{2,6}$) could be found at δ_C/δ_H 107.4/7.15–7.26 ppm, which was only shown in the spectra of AEOL-2 and AEOL-4. Finally, a considerably stronger signal for the condensed lignin structure was found at δ_C/δ_H 105.8/6.42 ppm in the spectrum of AEOL-6, indicating that autocatalyzed pretreatments at higher temperature led to more condensed lignin.

Quantification of the main lignin interunit linkages by 2D-HSQC NMR technique can evaluate the explicit structural evolution of AEOL under different pretreatment conditions [41]. The proportion of α-ethoxylated β-O-4′ linkages (A') increased with the pretreatment temperatures, reaching 69.13% in AEOL-4 and 82.13% in AEOL-6 (Table 5). This implied that the occurrence of α-ethoxylation was enhanced with increased temperature. In addition, the proportions of β-β′ and β-5′ linkages steadily decreased as pretreatment temperatures increased, reaching 11.01% and 1.55%, respectively, at 240 °C. The other noteworthy parameter, S/G ratio, was also calculated to investigate the change of lignin structure. The higher S/G ratios of AEOL-4 and AEOL-6 revealed that the lignins with more linear structures were separated at higher temperatures during the AEOP process. Due to the unavailable C5 position of the aromatic ring for cross-linked structures, high S/G ratio lignin (also called condensed lignin) shows a more linear structure [38]. Noticeably, the S/G ratios were higher than those calculated from Py-GC/MS, but the overall trend was consistent. This indicated that the demethoxylation of S units probably occurred during the pyrolysis of Py-GC/MS, leading to more G units, and thus, a decrease in the S/G ratio [42].

Table 5
Quantification of substructures from AEOL samples by 2D-HSQC NMR.

Lignin inter-unit linkages	Percentage (%)		
	AEOL-2	AEOL-4	AEOL-6
α-ethoxylated β-O-4′ aryl ethers (A')	39.43	69.13	82.13
β-O-4′ Aryl ethers (A)	38.28	15.19	5.31
β-β′ (Resinols) (B)	16.05	12.09	11.01
β-5′(Phenylcoumarans) (C)	6.24	3.59	1.55
S/G ratio[a]	1.6	2.1	2.7

[a] S/G ratio was obtained by the equation: S/G ratio = 0.5 $IS_{2,6}/IG_2$.

3.6.2. ^{31}P NMR spectra analyses

Quantitative ^{31}P NMR has been frequently used to investigate changes of the hydroxyl groups in lignin during pretreatment. The signals of carboxyl groups were detected at 135.7–134.0 ppm, while the signals of aliphatic hydroxyl groups were found at 148.5–146.1 ppm. It was found that AEOL-2 had the highest content of aliphatic hydroxyl groups, because it had the highest content of carbohydrates among the three samples, as revealed by the results of sugar analyses. The signals at 143.8–141.8, 140.4–138.6, and 138.5–137.0 ppm were assigned to syringyl hydroxyl groups, guaiacyl hydroxyl groups, and *p*-hydroxyphenyl hydroxyl groups, respectively. As seen in Table 6, the increase in temperature of the AEOP process was accompanied by an increase in the carboxylic hydroxyl groups and a decrease of phenolic hydroxyl groups. The previous investigation showed that phenolic hydroxyl content was the primary parameter that influences the antioxidant properties of lignin [9]. In this study, the content of phenolic hydroxyl groups in AEOL-2, AEOL-4, and AEOL-6 were 2.14, 1.95, and 1.90 mmol/g, respectively. The increase of the pretreatment temperature led to a reduction in the amount of total phenolic hydroxyl groups. As reported extensively in the literature, the scission of β-O-4′ linkages gives rise to more phenolic hydroxyl groups, while the oxidation of phenolic hydroxyl groups may result in the increased content of carboxylic groups [26]. In addition, the oxidation of aliphatic hydroxyl groups also resulted in the creation of carboxyl groups during the AEOP process [14]. These oxidation reactions could explain the decreased content of phenolic hydroxyl groups and the increased content of carboxyl hydroxyl groups in AEOL-6 and AEOL-4.

3.7. Antioxidant activity analyses

The antioxidant properties of AEOL were evaluated by three selected methodologies using the commercial antioxidant BHT as reference. The results of the DPPH and ABTS assays are expressed in terms of IC_{50} (half maximal inhibitory concentration), while the results of FRAP analyses are expressed as millimolar equivalents of $FeSO_4 \cdot 7H_2O$ per gram of lignin. The lower the IC_{50} or the higher the FRAP values, the higher the antioxidant properties of the AEOL samples tested.

Table 1 gives the calculated values for the AEOL samples, as well as for BHT. All lignin samples showed higher radical scavenging activity than BHT in DPPH assay, with IC_{50} values ranging from 78.00 to114.40 μg/mL. Michelin et al. [3] reported IC_{50} values of 0.17–0.26 mg/mL in DPPH assay and 0.016–0.028 mg/mL in ABTS assay for lignin from corncob recovered from a residue pretreated by liquid hot water and ethanol organosolv. Sun et al. [39] reported IC_{50} values in the range of 0.18–0.50 mg/mL in DPPH assay for lignin samples from the bamboo stem, which was extracted by alkali/alkaline ethanol pulping method after steam explosion pretreatment. Wen et al. [43] reported IC_{50} values of 110 mg/mL, 100 mg/mL, and 60 mg/mL (DPPH assay) for bamboo alkali lignin, milled wood lignin, and lignin isolated from DMSO/NMI (dimethylsulfoxide/*N*-methylimidazole) dissolved system, respectively. These different antioxidant properties of lignin samples indicated that the antioxidant properties of lignin were strongly influenced by the source of lignocellulosic material, the extraction methods employed, and the treatments applied during lignin separation and purification.

Table 6
Quantification of the AEOL samples by ^{31}P NMR.

Functional groups	Content (mmol/g)		
	AEOL-2	AEOL-4	AEOL-6
Aliphatic OH	2.91	1.56	1.15
Syringyl phenolic OH	0.35	0.79	0.81
Guaiacyl phenolic OH	1.67	1.05	0.99
p-Hydroxyphenyl phenolic OH	0.12	0.11	0.06
Carboxylic OH (COOH)	0.21	0.48	0.98
Total phenolic OH	2.14	1.95	1.90

As seen from the results of the DPPH and ABTS assays in Table 1, the pretreatment temperature had a negative correlation with the radical scavenging activity of AEOL (AEOL-1 to AEOL-6). It was reported that phenolic hydroxyl content was the primary parameter that influences the antioxidant properties of lignin, and the lignins with higher phenolic hydroxyl content showed higher antioxidant activity [9]. In this study, the negative correlation between pretreatment temperature and the radical scavenging activity of AEOL samples was in agreement with the phenolic hydroxyl group content in these samples. With lignin, researchers generally associate lower molecular weight with greater antioxidant activity [9,10]. Lignin with lower molecular weight suggested it contains more small lignin fragments which result from the cleavage of β-O-4′ linkages. The cleavage of β-O-4′ linkages led to the increased phenolic OH content, and then the lignin antioxidant activity increased. However, in the present work, the molecular weight of AEOL samples decreased with the pretreatment temperature, but the AEOL samples extracted at higher temperatures showed lower radical scavenging activity. The reason for this phenomenon was that some of the phenolic hydroxyl groups released by the scission of β-O-4′ linkages during the AEOP process were oxidized to carboxyl groups, as revealed by ^{31}P NMR analyses, and the carboxyl groups were not helpful for improving the antioxidant activity of lignin.

The antioxidant properties of lignin might depend on not only phenolic hydroxyl content and molecular weight but also side chain composition. According to previous reports, the presence of α-carbonyl groups in the aliphatic chain and carbon double bonds conjugated with aromatic rings have a negative influence on the antioxidant properties of lignin [22]. Compared with the AEOL separated at lower temperatures, AEOL separated at higher temperatures produced more pyrolysis compounds with α-carbonyl groups in the aliphatic chain (Table 4), such as 1-(2,6-dihydroxy-4-methoxyphenyl)-ethanone, 1-(4-Hydroxy-3,5-dimethoxyphenyl)-ethanone, 2,4,6-trihydroxy-3-methylbutyrophenone, and 3,5-dimethoxy-4-hydroxybenzaldehyde (structures 27, 47, 44, and 40, respectively; Fig. S5, Supporting information). These results supported the fact that the AEOL samples separated at higher pretreatment temperatures showed lower radical scavenging activity. The antioxidant activity of AEOL (AEOL-7 to AEOL-22) obtained with varied pretreatment times and ethanol concentrations presented a similar behavior separately, implying that the pretreatment time and ethanol concentration are not significant factors affecting the antioxidant activity of AEOL. The IC_{50} values of AEOL samples tested by ABTS assay were significantly lower than those calculated from the DPPH assay, but the overall trend is consistent. This could be explained by the difference in mechanisms of the lignin radical scavenging activity in the DPPH and ABTS assays. The ABTS test assesses scavenging activity by measuring electron or proton transfer, whereas the DPPH test measures the combination of electron and H atom transfer. In the case of the DPPH test, side reactions could hinder/slow radical scavenging activity [44].

For the FRAP assay, antioxidant activity occurs by the reduction of ferric iron (Fe^{3+}) to ferrous iron (Fe^{2+}) in the presence of antioxidants, which act as reductants for the half-reaction reduction potentials above Fe^{3+}/Fe^{2+}. In the present work, $FeSO_4 \cdot 7H_2O$ was taken as a standard and the FRAP activity of AEOL samples was calculated according to a linear calibration curve ($Y = 0.9536x - 0.0686$, $R^2 = 0.9959$). All the AEOL samples showed FRAP activity in the range of 2.18 mmol/g to 3.41 mmol/g, which was lower than that of BHT (3.63 mmol/g). The highest FRAP value was showed by AEOL-1 (3.41 mmol/g) followed by AEOL-20 (3.35 mmol/g) and AEOL-8 (3.27 mmol/g). The observed FRAP value of these three lignin might be due to the higher phenolic hydroxyl content as compared to other AEOL samples, as revealed by the analyses of ^{31}P NMR.

4. Conclusions

The structural features and antioxidant activity of lignin extracted from Chinese quince fruits by auto-catalyzed ethanol organosolv pretreatment were studied in detail. Different pretreatment conditions (temperature, time, and ethanol concentration) displayed a significant effect on the lignin yield. The maximum lignin yield (14.40%) was observed in the pretreatment conditions of 200 °C, 90 min, and 60% aqueous ethanol. GPC analyses proved that the molecular weight of the AEOL samples had a negative correlation with the temperature applied during its separation. The S/G ratios of the AEOL samples increased with the pretreatment temperature. The oxidation reaction resulted in decreased content of phenolic hydroxyl groups in the AEOL samples separated at high temperature. The antioxidant activity tests indicated the AEOL samples separated at lower temperature had a higher antioxidant activity that was similar to commercial antioxidant BHT. The results of antioxidant activity tests indicated the AEOL samples had the potential for use as natural antioxidants in the food industry.

Declaration of competing interest

The authors declare that there is no conflict of interests regarding the publication of this article.

Acknowledgements

We sincerely acknowledge the financial support of the National Natural Science Foundation of China (U1804111) and the Earmarked Fund for Modern Agro-industry Technology Research System (CARS14-1-29).

Appendix A. Supplementary data

Supplementary data to this article can be found online at https://doi.org/10.1016/j.ijbiomac.2020.08.249.

References

[1] J.C. del Río, P. Prinsen, J. Rencoret, L. Nieto, J. Jiménez-Barbero, Á.T. Ralph, A. Gutiérrez, Structural characterization of the lignin in the cortex and pith of elephant grass (*Pennisetum purpureum*) stems, J. Agric. Food Chem. 60 (2012) 3619–3634.
[2] P. Ortiz-Serna, M. Carsí, M. Culebras, M.N. Collins, M.J. Sanchis, Exploring the role of lignin structure in molecular dynamics of lignin/bio-derived thermoplastic elastomer polyurethane blends, Int. J. Biol. Macromol. 158 (2020) 1369–1379.
[3] M. Michelin, S. Liebentritt, A.A. Vicente, J.A. Teixeira, Lignin from an integrated process consisting of liquid hot water and ethanol organosolv: physicochemical and antioxidant properties, Int. J. Biol. Macromol. 120 (2018) 159–169.
[4] G.L. Catignani, M.E. Carter, Antioxidant properties of lignin, J. Food Sci. 47 (1982) 1745.
[5] V. Ugartondo, M. Mitjans, M.P. Vinardell, Comparative antioxidant and cytotoxic effects of lignins from different sources, Bioresour. Technol. 99 (2008) 6683–6687.
[6] J.H. Lora, W.G. Glasser, Recent industrial applications of lignin: a sustainable alternative to nonrenewable materials, J. Polym. Environ. 10 (2002) 39–48.
[7] K. Wörmeyer, T. Ingram, B. Saake, G. Brunner, I. Smirnova, Comparison of different pretreatment methods for lignocellulosic materials. Part II: influence of pretreatment on the properties of rye straw lignin, Bioresour. Technol. 102 (2011) 4157–4164.
[8] M.H. Hussin, A.M. Shah, A.A. Rahim, M.N.M. Ibrahim, D. Perrin, N. Brosse, Antioxidant and anticorrosive properties of oil palm frond lignins extracted with different techniques, Ann. For. Sci. 72 (2015) 17–26.
[9] X. Pan, J.F. Kadla, K. Ehara, N. Gilkes, J.N. Saddler, Organosolv ethanol lignin from hybrid poplar as a radical scavenger: relationship between lignin structure, extraction conditions, and antioxidant activity, J. Agric. Food Chem. 54 (2006) 5806–5813.
[10] A. García, A. Toledano, M.Á. Andrés, J. Labidi, Study of the antioxidant capacity of *Miscanthus sinensis* lignins, Process Biochem. 45 (2010) 935–940.
[11] A. Romaní, G. Garrote, F. Lopez, J.C. Parajo, *Eucalyptus globulus* wood fractionation by autohydrolysis and organosolv delignification, Bioresour. Technol. 102 (2011) 5896–5904.
[12] M. Brahim, N. Boussetta, N. Grimi, E. Vorobiev, I. Zieger-Devin, N. Brosse, Pretreatment optimization from rapeseed straw and lignin characterization, Ind. Crop. Prod. 95 (2017) 643–650.
[13] Y. Guo, J. Zhou, J. Wen, G. Sun, Y. Sun, Structural transformations of triploid of Populus tomentosa Carr. lignin during auto-catalyzed ethanol organosolv pretreatment, Ind. Crop. Prod. 76 (2015) 522–529.
[14] J. Wen, B. Xue, S. Sun, R. Sun, Quantitative structural characterization and thermal properties of birch lignins after auto-catalyzed organosolv pretreatment and enzymatic hydrolysis, J. Chem. Technol. Biotechnol. 88 (2013) 1663–1671.
[15] Y. Hamauzu, Y. Mizuno, Non-extractable procyanidins and lignin are important factors in the bile acid binding and radical scavenging properties of cell wall material in some fruits, Plant Foods Hum. Nutr. 66 (2011) 70–77.
[16] Y. Hamauzu, N. Takedachi, R. Miyasaka, H. Makabe, Heat treatment of Chinese quince polyphenols increases rat plasma levels of protocatechuic and vanillic acids, Food Chem. 118 (2010) 757–763.
[17] L. Wang, H.M. Liu, C.Y. Zhu, A.J. Xie, Y.X. Ma, P.Z. Zhang, Chinese quince seed gum: flow behaviour, thixotropy and viscoelasticity, Carbohydr. Polym. 209 (2019) 230–238.
[18] Z. Qin, X. Wang, H. Liu, D. Wang, G. Qin, Structural characterization of Chinese quince fruits lignin pretreated with enzymatic hydrolysis, Bioresour. Technol. 262 (2018) 212–220.
[19] M. Li, S. Sun, F. Xu, R. Sun, Formic acid based organosolv pulping of bamboo (*Phyllostachys acuta*): comparative characterization of the dissolved lignins with milled wood lignin, Chem. Eng. J. 179 (2012) 80–89.
[20] A. Sluiter, B. Hames, R. Ruiz, C. Scarlata, J. Sluiter, D. Templeton, D. Crocker, Determination of Structural Carbohydrates and Lignin in Biomass, NREL-LAP. Technical Report NREL/TP-510-42618, 2008.
[21] H. Sadeghifar, T. Wells, R.K. Le, F. Sadeghifar, J. Yuan, A. Jonas Ragauskas, Fractionation of organosolv lignin using acetone: water and properties of the obtained fractions, ACS Sustain. Chem. Eng. 5 (2016) 580–587.
[22] Z. Qin, Z. Zhang, H. Liu, G. Qin, X. Wang, Acetic acid lignins from Chinese quince fruits (*Chaenomeles sinensis*): effect of pretreatment on their structural features and antioxidant activities, RSC Adv. 8 (2018) 24923–24931.
[23] A. Barapatre, A.S. Meena, S. Mekala, A. Das, H. Jha, In vitro evaluation of antioxidant and cytotoxic activities of lignin fractions extracted from Acacia nilotica, Int. J. Biol. Macromol. 86 (2016) 443–453.
[24] V. Baltrušaitytė, P.R. Venskutonis, V. Čeksterytė, Radical scavenging activity of different floral origin honey and beebread phenolic extracts, Food Chem. 101 (2007) 502–514.
[25] G. Vázquez, E. Fontenla, J. Santos, M.S. Freire, J. González-Álvarez, G. Antorrena, Antioxidant activity and phenolic content of chestnut (*Castanea sativa*) shell and eucalyptus (*Eucalyptus globulus*) bark extracts, Ind. Crop. Prod. 28 (2008) 279–285.
[26] J. Wildschut, A.T. Smit, J.H. Reith, W.J.J. Huijgen, Ethanol-based organosolv fractionation of wheat straw for the production of lignin and enzymatically digestible cellulose, Bioresour. Technol. 135 (2013) 58–66.
[27] L.-Y. Liu, S.C. Patankar, R.P. Chandra, N. Sathitsuksanoh, J.N. Saddler, S. Renneckar, Valorization of bark using ethanol-water organosolv treatment: isolation and characterization of crude lignin, ACS Sustain. Chem. Eng. 8 (2020) 4745–4754.
[28] L.V.A. Gurgel, M.T.B. Pimenta, A.A.S. Curvelo, Ethanol-water organosolv delignification of liquid hot water (LHW) pretreated sugarcane bagasse enhanced by high-pressure carbon dioxide (HP-CO_2), Ind. Crop. Prod. 94 (2016) 942–950.
[29] Y. Ni, Q. Hu, Alcell® lignin solubility in ethanol-water mixtures, J. Appl. Polym. Sci. 57 (1995) 1441–1446.
[30] Z. Qin, Y. Ma, H. Liu, G. Qin, X. Wang, Structural elucidation of lignin-carbohydrate complexes (LCCs) from Chinese quince (*Chaenomeles sinensis*) fruits, Int. J. Biol. Macromol. 116 (2018) 1240–1249.
[31] S. Dapía, V. Santos, J.C. Parajó, Study of formic acid as an agent for biomass fractionation, Biomass Bioenergy 22 (2002) 213–221.
[32] X. Zhao, K. Cheng, D. Liu, Organosolv pretreatment of lignocellulosic biomass for enzymatic hydrolysis, Appl. Microbiol. Biotechnol. 82 (2009) 815–827.
[33] Y. Bai, L. Xiao, Z. Shi, R. Sun, Structural variation of bamboo lignin before and after ethanol organosolv pretreatment, Int. J. Mol. Sci. 14 (2013) 21394–21413.
[34] J. Ren, Q. Li, F. Dong, Y. Feng, Z. Guo, Phenolic antioxidants-functionalized quaternized chitosan: synthesis and antioxidant properties, Int. J. Biol. Macromol. 53 (2013) 77–81.
[35] A.S. Jääskeläinen, Y. Sun, D.S. Argyropoulos, T. Tamminen, B. Hortling, The effect of isolation method on the chemical structure of residual lignin, Wood Sci. Technol. 37 (2003) 91–102.
[36] M.N.M. Ibrahim, N. Zakaria, C.S. Sipaut, O. Sulaiman, R. Hashim, Chemical and thermal properties of lignins from oil palm biomass as a substitute for phenol in a phenol formaldehyde resin production, Carbohydr. Polym. 86 (2011) 112–119.
[37] N. Ramezani, M. Sain, Thermal and physiochemical characterization of lignin extracted from wheat straw by organosolv process, J. Polym. Environ. 26 (2018) 3109–3116.
[38] J. Wen, S. Sun, B. Xue, R. Sun, Recent advances in characterization of lignin polymer by solution-state nuclear magnetic resonance (NMR) methodology, Materials 6 (2013) 359–391.
[39] S. Sun, J. Wen, M. Ma, R. Sun, G.L. Jones, Structural features and antioxidant activities of degraded lignins from steam exploded bamboo stem, Ind. Crop. Prod. 56 (2014) 128–136.
[40] S. Bauer, H. Sorek, v.D. Mitchell, A.B. Ibáñez, D.E. Wemmer, Characterization of *Miscanthus giganteus* lignin isolated by ethanol organosolv process under reflux condition, J. Agric. Food Chem. 60 (2012) 8203–8212.
[41] H. Yin, H. Liu, Y. Liu, Structural characterization of lignin in fruits and stalks of Chinese Quince, Molecules 22 (2017) 890–903.
[42] P.F.V. Bergen, I. Poole, T.M.A. Ogilvie, Evidence for demethylation of syringyl moieties in archaeological wood using pyrolysis-gas chromatography/mass spectrometry, Rapid Commun. Mass Spectrom. 14 (2000) 71–79.
[43] J.-L. Wen, B.-L. Xue, F. Xu, R.-C. Sun, A. Pinkert, Unmasking the structural features and property of lignin from bamboo, Ind. Crop. Prod. 42 (2013) 332–343.
[44] D. Huang, B. Ou, R.L. Prior, The chemistry behind antioxidant capacity assays, J. Agric. Food Chem. 53 (2005) 1841–1856.